




## Article

# Synthesis and optimization of a montmorillonite-tolerant zwitterionic polycarboxylate superplasticizer *via* Box-Behnken design

Jun Ren<sup>1,2</sup> , Shuqiong Luo<sup>3\*</sup>, Shi Shi<sup>4</sup>, Hongbo Tan<sup>5</sup>, Xianfeng Wang<sup>2</sup>, Min Liu<sup>2</sup> and Xiangguo Li<sup>5</sup>

<sup>1</sup>School of Architecture and Planning, Yunnan University, Kunming, 650051, P.R. China; <sup>2</sup>Guangdong Key Laboratory of Durability in Coastal Civil Engineering, College of Civil Engineering, Shenzhen University, Shenzhen, 518060, P.R. China; <sup>3</sup>Henan Key Laboratory of Materials on Deep-Earth Engineering, School of Materials Science and Engineering, Henan Polytechnic University, Jiaozuo 454003, P.R. China; <sup>4</sup>Department of Civil, Environmental and Geomatic Engineering, University College London, London, WC1E 6BT, UK and <sup>5</sup>State Key Laboratory of Silicate Materials for Architectures, Wuhan University of Technology, Wuhan 430070, P.R. China

### Abstract

Polycarboxylate superplasticizer (PCE) is sensitive to the clay present in concrete aggregates. In particular, Montmorillonite (Mnt), an impurity inevitably contained in the aggregate, can significantly influence the performance of concrete. In an effort to improve the compatibility of PCE, a zwitterionic PCE with cationic amide groups and shorter side-chain lengths was synthesized *via* free radical copolymerization. The optimal synthesis condition was verified *via* Box-Behnken design. In addition to characterizing the PCE, the performance of PCE in cement pastes with or without Na-Mnt was examined and the underlying mechanism was explored. The results show that, compared with commercially available PCE, the required dosage of PCE for cements containing Na-Mnt decreased. Unlike commercially available PCE, no intercalation occurred on the newly manufactured clay-tolerant PCE within the layers of Mnt, resulting in a greater sorption thickness and improved dispersion of the cements containing Na-Mnt.

**Keywords:** cement, clay, intercalation, montmorillonite (Mnt), polycarboxylate superplasticizer, sorption

(Received 2 November 2020; revised 11 July 2021; Accepted Manuscript online: 21 July 2021; Associate Editor Chun-Hui Zhou)

The demand for high-/ultra-high-performance concrete has increased dramatically in recent years, creating demand for high-quality aggregates (Wang *et al.*, 2017; Rashad, 2018; Zhang *et al.*, 2019). This demand cannot be fully met due to the depletion of natural resources, including natural sand and gravel (Ioannidou *et al.*, 2017). Aggregates contaminated by impurities such as clay and silt rather than gravel or sand are typically utilized in this regard.

Various organic chemicals have been applied in clays in efforts to enhance their efficiency, and the interactions between them have been studied (Li *et al.*, 2019; Tan *et al.*, 2019; Guo *et al.*, 2020; Shen *et al.*, 2020; Zhang *et al.*, 2020). One of the most important chemical admixtures, polycarboxylate superplasticizers (PCEs), is a type of clay-sensitive superplasticizer. However, contamination by clay or silt makes PCE inherently incompatible with aggregates (Wala & Rosiek, 2003; Dziekan *et al.*, 2011; Ren *et al.*, 2019, 2021; Tan *et al.*, 2018a). This negatively impacts the dispersion of PCE and the workability and pumping ability of the concrete (Lei & Plank, 2012b).

There has been extensive research to date conducted on the incompatibility between PCE and clay (Sánchez-Martín *et al.*,

2008; Ng & Plank, 2012; Zhao *et al.*, 2017; Gao *et al.*, 2018; Ma *et al.*, 2020). It is generally accepted that the greater sorption of PCE on clay is due to the larger specific surface of clay grains. Clay minerals have a layered structure with two Si tetrahedra and one Al oxide octahedron in between (2:1 structure), or one Si tetrahedron and one Al oxide octahedron (1:1 structure). Upon contact with water, some 2:1 clay minerals, such as smectite, swell because of expansion of the interlayer space (Tregger *et al.*, 2010; Tan *et al.*, 2018a). Therefore, the polyethylene oxide (PEO) side-chains can easily become inserted into the interlayer, causing disjunction in the cement particle dispersal with steric repulsion (Suter & Coveney, 2009; Tan *et al.*, 2016a).

Adding small-molecule sacrificial agents such as poly(vinyl alcohol) or cationic surfactants may resolve the incompatibility issue (Nehdi, 2014; Wang *et al.*, 2015; Tan *et al.*, 2018b). Introducing novel PCE structures may also be effective (Chen *et al.*, 2018; Tang *et al.*, 2020). The three main approaches to such modifications include increasing the steric hindrance of PCE, introducing a cationic group to produce an amphoteric copolymer and using no PEO side-chains. Xu *et al.* (2018) synthesized quaternary PCEs grafted with  $\beta$ -cyclodextrin by copolymerizing the monovinyl  $\beta$ -cyclodextrin monomer, sodium methylallyl sulfonate, acrylic acid and methyl allyl polyoxyethylene ether (TPEG) *via* free-radical polymerization initiated by hydrogen peroxide solution to improve the performance of a kaolin clay. Liu *et al.* (2017) used star-shaped PCE synthesized by acrylic acid-methyl allyl polyoxyethylene ether (AA-TPEG) copolymer arms on a polyol(pentaerythritol) core to minimize the detrimental

\*E-mail: luoshuqiong@hpu.edu.cn

This paper was submitted for the special issue 'Clays and Functional Materials' and was presented at the Asian Clay Conference, Singapore 2020.

**Cite this article:** Ren J, Luo S, Shi S, Tan H, Wang X, Liu M, Li X (2021). Synthesis and optimization of a montmorillonite-tolerant zwitterionic polycarboxylate superplasticizer *via* Box-Behnken design. *Clay Minerals* 56, 117–125. <https://doi.org/10.1180/clm.2021.25>

effects of clays in cement. These methods are mainly based on increasing the size of PCE. Li *et al.* (2016) employed the zwitterionic monomer 3-(2-(methacryloyloxy)ethyl)dimethylammonio-propane-1-sulfonate (DMAPS) to prepare a novel amphiphilic polycarboxylate copolymer that may be adsorbed on a clay surface without intercalation.

There have been many other valuable contributions to this literature. Lei & Plank (2012a, 2014b) prepared a series of PCEs with hydroxy alkyl lateral chains from methacrylic acid and hydroxyl-alkyl methacrylate esters that performed well on dispersing cement with Na-montmorillonite (Na-Mnt; Warr, 2020), as they did not intercalate into its layered structure. The same authors also attempted to modify the PCE side-chain by synthesizing a series of vinyl ether-based PCEs containing two monomers: maleic anhydride and 4-hydroxybutyl vinyl ether. The PCE exhibited high cement dispersion ability due to the lack of intercalation with the clay. Xing *et al.* (2016) induced the tertiary amino group from 2-(dimethylamino)ethyl methacrylate as the end group of a side-chain to prepare terpolymer PCEs from acrylic acid and itaconic acid, which showed enhanced sorption on the clay surface by eliminating the intercalation of the PEO side-chain.

The clay-tolerance properties of modified PCEs can be significantly enhanced using the above methods, but the polymerization of chemicals with introduced functional groups requires accurate control over the sophisticated synthesis procedure. Considering its cost, there is demand for novel synthesis techniques for clay-tolerant PCEs (ct-PCEs) based on the conventional PCE. Previous studies have generally involved trial and error rather than precise optimization processes. Compared to traditional experimental methods, response surface methodologies such as Box-Behnken design (BBD) or central composite design (CCD) provide a systematic, efficient strategy to correlate the interactive effects of numerous parameters simultaneously through statistical procedures (Ren *et al.*, 2019).

In the present study, a zwitterionic PCE with cationic amide groups and shorter side-chain lengths was synthesized *via* copolymerization. Because montmorillonite (Na-Mnt) has been identified as the most important mineral composition of the clay (Lei & Plank, 2014a), performance-based optimization of the synthesis conditions of the ct-PCE was conducted by determining the fluidity of the cement paste containing Na-Mnt *via* BBD. Gel permeation chromatography (GPC), dynamic light scattering (DLS) and Fourier-transform infrared (FTIR) spectroscopy were used to characterize the physicochemical properties of the optimized ct-PCE. The interactions between the sample materials were investigated by total organic carbon (TOC) analysis, X-ray photoelectron spectroscopy (XPS) and X-ray diffraction (XRD) with regards to the sorption amount, sorption thickness and intercalation of the ct-PCE in Na-Mnt.

## Materials

The P.O. 42.5 Cement (PC) (which meets the Chinese standard GB175-2007) used in this study was supplied by China United Cement Co. Ltd. The Na-Mnt with a specific surface area of  $24.86 \text{ m}^2 \text{ g}^{-1}$  was supplied by Shenzhen Huanan Xinyang Tech. Co. Ltd, China. The typical chemical compositions of the PC and clay are listed in Table 1.

Allyl polyethylene glycol (APEG) (commercial product, purity  $\geq 99.0\%$ ) with various molecular weight of 500, 1000, 2000 and 2400 Da was supplied by Nantong Jinlai Chemical Co. Ltd, China, as the side-chain. All chemicals used for polymerization, including

**Table 1.** Chemical composition (wt.%) of the PC and clay.

	CaO	SiO <sub>2</sub>	Al <sub>2</sub> O <sub>3</sub>	MgO	Na <sub>2</sub> O	SO <sub>3</sub>	Fe <sub>2</sub> O <sub>3</sub>	K <sub>2</sub> O	LOI
Cement	64.35	21.79	4.45	2.38	N/A	2.45	3.55	0.38	1.50
Na-Mnt	2.17	72.35	13.92	2.13	5.22	N/A	1.17	0.41	0.51

LOI = loss on ignition.

acrylic acid (AA), methylacrylamide (AM), diallyldimethylammonium chloride potassium (DMAAC), 2-acrylamido-2-methyl-1-propanesulfonic acid (AMPS), 2-mercaptoethanol (TGA), potassium persulfate (KPS) and sodium hydroxide (NaOH), were of reagent grade and were supplied by Sinopharm Chemical Reagent Co., Ltd, China. A commercial PCE (c-PCE) from Jiangsu China Railway ARIT New Materials Co., Ltd, was employed for comparison.

## Experimental

### Polymerization

The ct-PCE used in this study was synthesized *via* free radical polymerization. APEG and water were added to a 500 mL four-neck round-bottomed flask and magnetically stirred while being heated to the target temperature. The monomer solution was added slowly and evenly as a solution containing the designated KPS dosage and a fixed amount of TGA (0.5 wt.% of the total weight of all monomers) was added. After the addition of all materials in the solution, polymerization proceeded under constant temperature for another 3 h followed by cooling to ambient temperature. The final PCE product was neutralized by NaOH solution to a pH of 7.

### Characterization

The molecular weight and molecular distribution, expressed as a polydispersity index (PDI), of PCE were determined by GPC (Wyatt Technology Corporation) with 0.1 M NaNO<sub>3</sub> as the eluent and poly(ethylene glycol) (PEG) as the standard. The conversion of the PCE was calculated from GPC results based on a previously reported technique (Sun *et al.*, 2016). Deionized water was used throughout the experiments. The chemical structure of the PCE was determined by FTIR spectroscopy (Nicolet Instruments, Inc., USA) using the KBr method in the range from 400 to 4000 cm<sup>-1</sup>. The hydrodynamic radii ( $R_h$ ) of the PCE were measured by DLS (Malvern Zetasizer Nano ZS) at 25°C.

### Test procedure

#### Sample preparation

To evaluate the dispersion performance of the superplasticizer, a cementitious paste containing 3% Na-Mnt was prepared at a water-to-cementitious material ratio of 0.29. The PCE dosage was controlled to 0.25% by weight of cementitious materials.

#### Dispersion of cementitious material

The dispersion ability of the PCE was determined *via* the fluidity of the pastes containing cement and Na-Mnt with a minislump test in accordance with Chinese standard GB/T 8077-2012.

#### Sorption on Na-Mnt

The sorption on Na-Mnt was measured using the depletion method, in which 0.5 g of Na-Mnt and 26.5 g of the synthetic

cement pore solution (prepared by dissolving 1.72 g  $\text{CaSO}_4 \cdot 2\text{H}_2\text{O}$ , 4.76 g  $\text{K}_2\text{SO}_4$ , 6.96 g  $\text{Na}_2\text{SO}_4$  and 7.12 g KOH in 1 L of deionized water; Lei & Plank, 2012a) with various PCE concentrations were poured into a 100 mL container and stirred for 9 min. The sorption of PCE on Na-Mnt was determined by means of TOC analysis (Shimadzu, Japan). A two-stage centrifugation was conducted to separate the solid phase and the aqueous phase. The solution was centrifuged at 3500 rpm for 15 min and then the resulting supernatant was further centrifuged at 12,000 rpm for another 15 min. The supernatant was decanted and diluted with deionized water for TOC analysis. The PCE sorption amount was calculated based on the change in the amount of superplasticizer from before vs after it contacted the binder, which was calculated from the TOC results.

#### Intercalation with Na-Mnt

X-ray diffraction was employed to examine the  $d$  spacing and the interlayer spacing of Na-Mnt (Tan *et al.*, 2016a) after hydrating the Na-Mnt specimens for 12 min. Following Xing *et al.* (2016), 0.56 g of clay and 24.56 g of synthetic cement pore solution prepared as described in the previous section with 0.25 wt.% of the tested PCE were added to a 50 mL container. The suspension was stirred for 10 min and centrifuged at 12,000 rpm for another 15 min. The solid was vacuum dried at 45°C for 48 h, followed by selection with a 200-mesh sieve. A Rigaku X-ray diffractometer with a Cu tube (Cu- $K\alpha$  radiation) was used to characterize the samples. The XRD traces were recorded over the 3–25°2 $\theta$  range at a speed of 4°2 $\theta$  min<sup>-1</sup> and a step size of 0.02°2 $\theta$ .

Dried solid powders were prepared for XPS measurements (Thermo Scientific K-Alpha, Thermo Fisher Ltd, USA) to test for Si and Ca elements. Aluminium was used as an anode target and the energy resolution was 0.05 eV. The sorption layer thickness of the PCEs was estimated by calculation of Si2p (Ji *et al.*, 2012; Tan *et al.*, 2016b).

#### Experimental parameters

Based on the literature review and preliminary tests, four factors were identified as the most significant in terms of chemical structure. The performance of ct-PCE was analysed according to these factors. The effects of the four factors, namely side-chain ratio (mole ratio between monomer and macromonomer), monomer ratio (mole ratio between AA and AM), initiator dosage (weight percentage of macromonomers and monomers) and synthesis temperature, on the polymerization of ct-PCE were observed and subsequently optimized (Table 2). Three levels were selected for each factor – lower, middle and higher, coded as -1, 0 and 1, respectively. A statistical response model of the initial minislump was quantitatively established for mathematical optimization. The analysis was conducted using the *Design Expert* software (Stat-Ease, Inc., USA).

## Results and discussion

#### Effect of PCE structure on cement with Na-Mnt minislump

The minislump of the Na-Mnt-blended cement incorporated with PCEs composed of various cationic anchor groups was determined and compared with c-PCE (Fig. 1a). A  $p$ -value of <0.05 was considered to be statistically significant. Introduction of the cationic group appears to have significantly increased the minislump of the paste, indicating that the ct-PCE

**Table 2.** Parameters for the experimental design.

Factor	Parameter	Unit	Symbol	Levels		
				Lower (-1)	Middle (0)	Higher (1)
A	Side-chain ratio	N/A	SR	1	3	5
B	Monomer ratio	N/A	MR	5	10	15
C	Initiator dosage	%	ID	1	2	3
D	Temperature	°C	T	50	70	90

performed better at dispersing the cement with the Na-Mnt impurity than c-PCE. The introduced cationic groups promoted electro-attraction between PCE and the negatively charged Mnt surface. Therefore, introducing cationic anchor groups improved the minislump of the sample and AM showed the best performance. The lower value of PCE with AMPS and DMDAAC may be attributed to steric hindrance from the methyl groups.

The side-chain length (molecular weights of 500, 1000, 2000 and 2400 Da) affects the minislump of the Na-Mnt-containing cement paste because there are statistically significant differences between the various PCEs (Fig. 1b). Compared to c-PCE, the minislump of the paste mixed with PAA-AM-APEG was greater, indicating that PCE copolymerizing AA, AM and APEG has greater Mnt tolerance. The side-chain significantly influenced the performance of PAA-APEG as well. The minislump spread increased when decreasing the side-chain length to give molecular weight of 2400 to 500 g mol<sup>-1</sup> and reached its greatest value when the side-chain length gave a molecular weight of 500 Da.

Although it is generally agreed that a greater side-chain length benefits the dispersion ability of PCE, the intercalation of the PEO side-chain into the interlayer of Mnt also causes dysfunction in the steric repulsion of PCE. In this case, a shorter side-chain led to a greater minislump.

#### Performance-based optimization of zwitterionic PCE

Box-Behnken design was employed to establish the optimal levels of four selected factors, namely side chain ratio (A), monomer ratio (B), initiator dosage (C) and synthesis temperature (D), which significantly affect the chemical structure and performance of ct-PCE. Twenty-four tests at factorial points and five repeated tests at central points were run in *Design Expert* software. The minislump spread was set as the response for determining the above four factors of PCE in dispersing cement with 3% Na-Mnt.

Equation 1 was generated based on the best-fitting model assessed by the software; it is a quadratic equation of the minislump (Y) as the response surface for the results and is visualized as a three-dimensional response surface plot (Fig. 2).

$$Y_1 = 260.00 + 12.17A + 3.25B + 2.33C + 1.58D - 3.25AB - 1.75AC - 1.50AD - 0.75BC + 0.25BD + 2.50CD + 4.83A^2 - 12.04B^2 + 4.83C^2 + 6.21D^2 \quad (R^2 = 0.9233) \quad (1)$$

The maximal minislump of the Na-Mnt-incorporated cement with PCE was set as the target to optimize the dispersion performance of ct-PCE. The maximal minislump (286 mm) was achieved with a side-chain ratio ((AA + AM):APEG) of 4.9, a

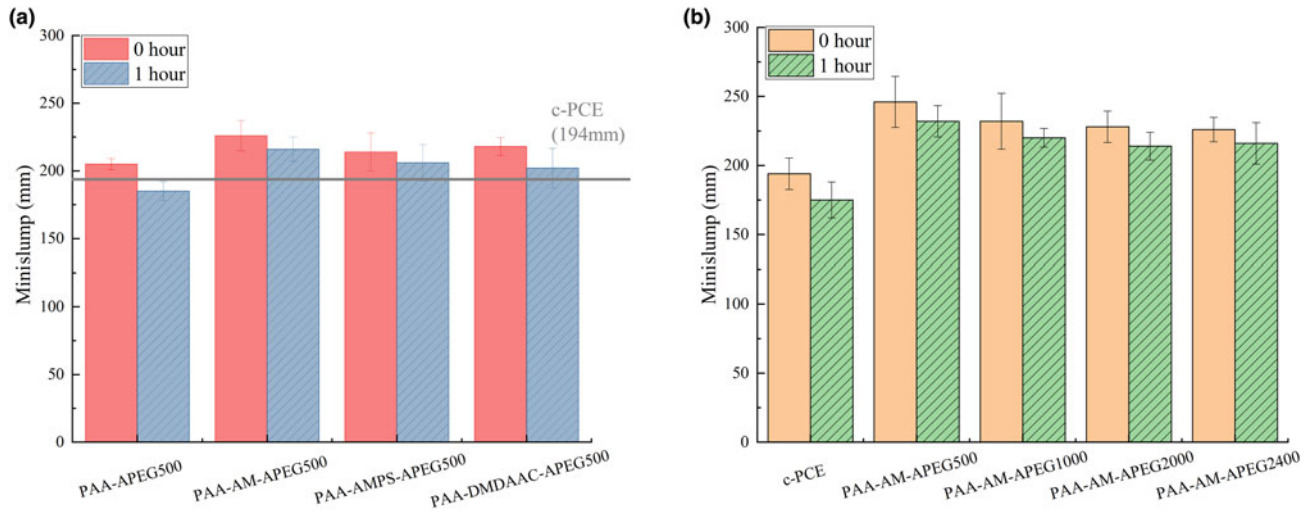


**Fig. 1.** Effects of PCEs with various chemical structures on initial minislump of cement paste including 3% Na-Mnt. (a) Effects of cationic anchor group and (b) effects of side-chain length.

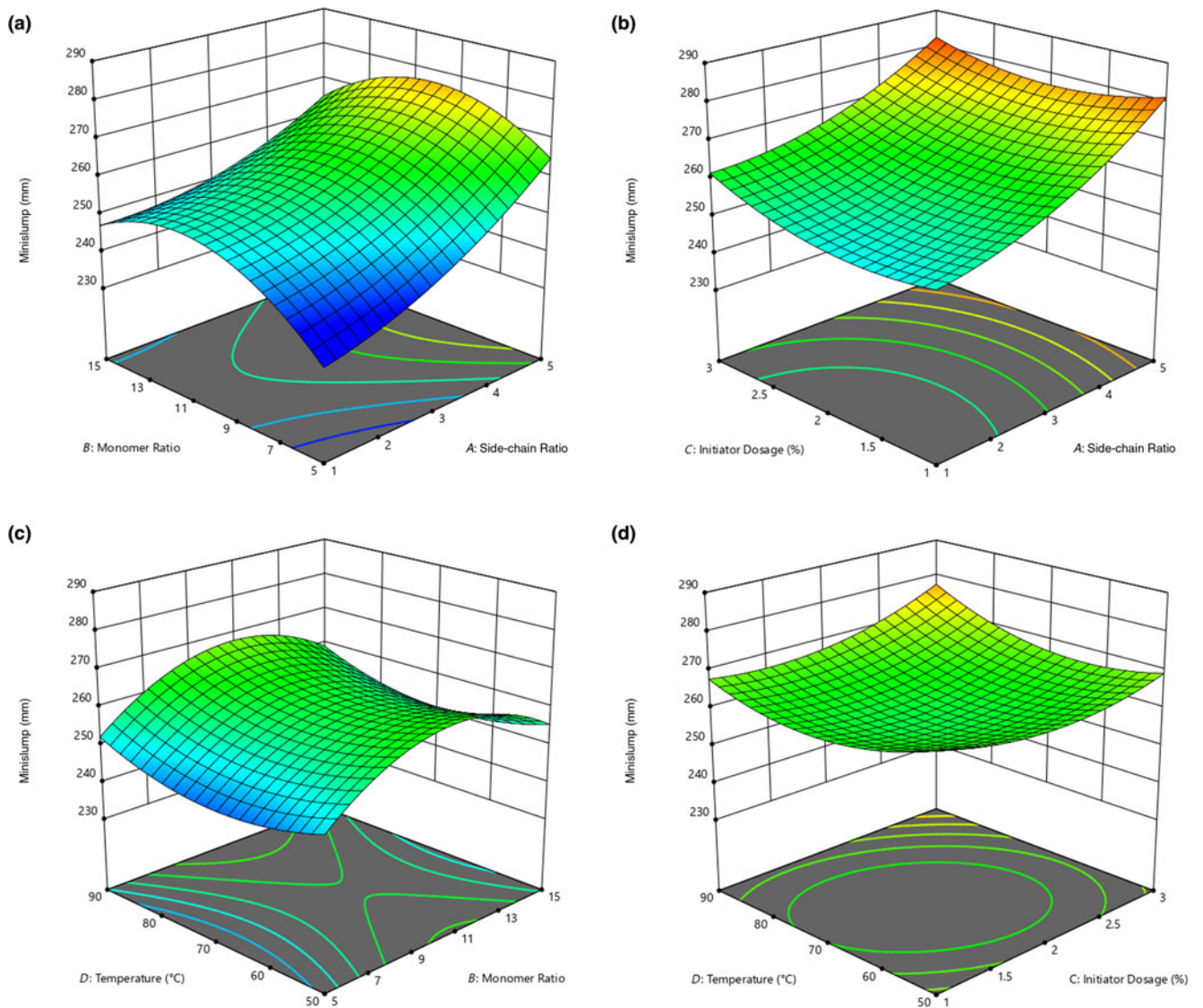


**Fig. 2.** Three-dimensional response surface plot of minislump of Na-Mnt-incorporated cement with ct-PCE in relation to (a) side-chain ratio and monomer ratio, (b) side-chain ratio and initiator dosage, (c) monomer ratio and synthesis temperature and (d) initiator dosage and synthesis temperature.

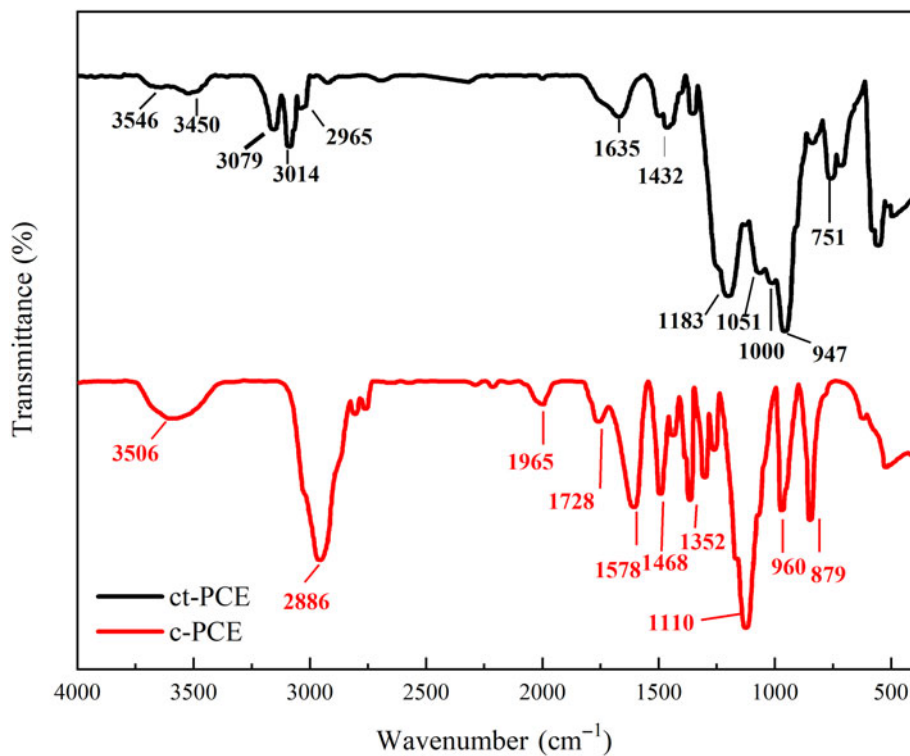


Fig. 3. FTIR spectra of ct-PCE and c-PCE.

Table 3. Molecular information for the ct-PCE and c-PCE samples.

Sample	$M_w$ (g mol <sup>-1</sup> )	$M_n$ (g mol <sup>-1</sup> )	PDI	$R_h$ (nm)
ct-PCE	23,576	10,273	2.29	5.25
c-PCE	28,785	11,287	2.55	6.59

$M_n$  = number-average molecular weight;  $M_w$  = mass-average molecular weight;  $R_h$  = hydrodynamic radii.

monomer ratio (AA:AM) of 9.8, an initiator dosage of 2.9% and a synthesis temperature of 81°C. Experiments were conducted using the optimized levels to check for differences between the experimental and the calculated values. The experimental value was  $277 \pm 15$  mm, which was  $96.86 \pm 0.05\%$  of the predicted value. Thus, the optimization model was considered accurate.

### Chemical properties of PCE

The FTIR spectra of both ct-PCE and c-PCE are shown in Fig. 3. For c-PCE, the bands at  $\sim 3506$  cm<sup>-1</sup> represented the O–H stretching band of carboxylate. Bands at 1965, 1728, 1578 and 1352 cm<sup>-1</sup> might be attributed to carbon–oxide bonds in carboxyl groups. Bands at 1110 and 879 cm<sup>-1</sup> were attributed to the C–O–C bond in polyether and the PEO side-chain. For ct-PCE, in addition to the bands at 3450, 2965 and 1635 cm<sup>-1</sup> for the carboxyl group and that at 1000 cm<sup>-1</sup> for the APEG side-chain, the bands at 3546, 1183 and 1051 cm<sup>-1</sup> confirmed that the cationic amide group was successfully grafted to ct-PCE.

GPC was used to characterize the molecular weight and weight distribution of ct-PCE and c-PCE. For comparison, the molecular information is presented in Table 3. The ct-PCE showed a smaller

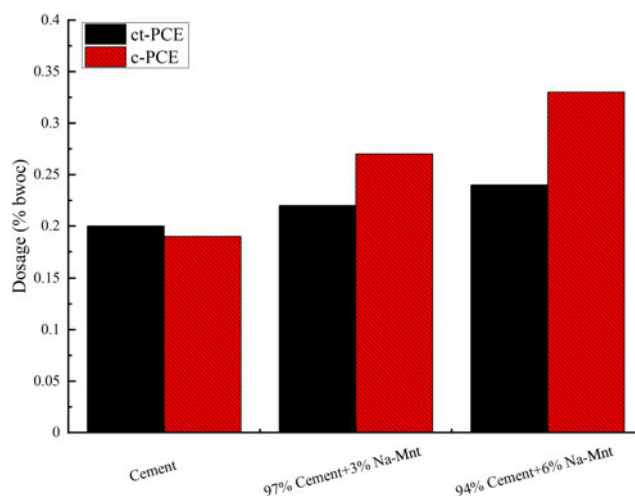


Fig. 4. Dosages of PCE required to achieve a minislump of  $260 \pm 5$  mm (water-to-cementitious material ratio = 0.29). bwoc = by weight of cementitious materials.

molecular weight than c-PCE, potentially due to the introduced shorter side-chain by APEG 500. However, for c-PCE, the materials often employed are macromonomers with molecular weights of  $\sim 2400$  Da. The smaller PDI of ct-PCE further suggests that the synthesized terpolymer has a uniform molecular weight distribution. The ct-PCE sample also shows greater conversion than c-PCE. The configuration of PCE expressed by the hydrodynamic radius from the DLS test is shown in Table 3, where ct-PCE had a smaller hydrodynamic radius, probably due to the small side-chain.

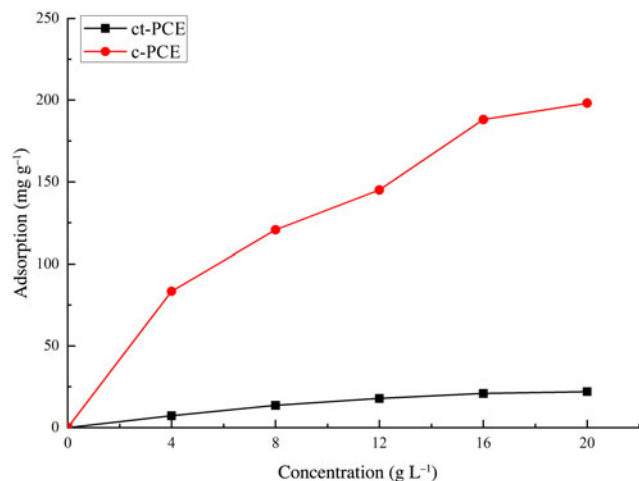


Fig. 5. Amount of ct-PCE and c-PCE sorbed on Na-Mnt.

### PCE dosage requirement

The effect of ct-PCE on the workability of cement containing Na-Mnt was investigated by determining the dosage requirement. The dosages of PCEs to achieve a minislump spread of  $260 \pm 5$  mm were determined accordingly. The results that statistically differed among different samples ( $p < 0.05$ ) are shown in Fig. 4. In the absence of Na-Mnt, the required dosage of ct-PCE was greater than that of c-PCE because the reduced side-chain hindered the steric repulsion of the PCE (Ran *et al.*, 2009). The required dosage of both PCEs increased with increasing Na-Mnt dosage.

There was a dramatic increase in PCE dosage observed with c-PCE compared to ct-PCE, which indicated that the compatibility of c-PCE with clay was poor due to intercalation with the PEO side-chain (Tan *et al.*, 2016a). A greater dosage was required for the cement without Na-Mnt compared to the cement with c-PCE, implying poor dispersion ability. However, there was no significant increase in the required amount of ct-PCE in the

presence of Na-Mnt, suggesting enhanced clay tolerance in the ct-PCE.

### Sorption of PCE on Na-Mnt

The interaction between PCE and Mnt was studied by sorption measurements (Fig. 5). The PCE samples, and specifically ct-PCE, displayed Langmuir-type adsorption, which significantly increased at lower dosages, reaching equilibrium plateau at higher dosages. In addition, an extremely high sorption of commercial PCE with the short PEO side-chains on Na-Mnt (up to  $200 \text{ mg g}^{-1}$  Na-Mnt) was observed, while only a small amount of the ct-PCE was sorbed ( $<25 \text{ mg}$ ) on Na-Mnt. Less adsorption was observed in ct-PCE, but a smaller required amount of ct-PCE was also observed (see the ‘PCE dosage requirement’ section), indicating the improved dispersion ability in ct-PCE. Both the c-PCE and Mnt have negative  $\zeta$ -potentials (Zadaka *et al.*, 2010), so the high observed sorption of c-PCE may be attributed to the PEO side-chain intercalating in the interlayer space (Ng & Plank, 2012; Tan *et al.*, 2016a). Considering that PCE intercalation does not improve the dispersion of cement particles (Flatt & Houst, 2001), it was not surprising that greater sorption led to poor dispersion.

### Intercalation behaviour of PCE with Na-Mnt

The XRD traces of Na-Mnt with or without PCE are plotted in Fig. 6. Without adding PCE, the  $d_{001}$ -spacing of Na-Mnt was  $\sim 1.23 \text{ nm}$  (Tambach *et al.*, 2004). After c-PCE was incorporated with long PEO side-chains, the  $d_{001}$ -spacing increased to  $1.73 \text{ nm}$ , implying that the PEO side-chains of c-PCE were intercalated into the interlayer space of the clay (Ng & Plank, 2012). However, there was no shift in the  $d$ -spacing after the addition of ct-PCE, indicating that there was no intercalation of ct-PCE in Na-Mnt. Therefore, the synthesized ternary ct-PCE did not intercalate in the Na-Mnt.

The thicknesses of the adsorption layers of both ct-PCE and c-PCE on Na-Mnt were calculated from Si2p XPS (Table 4).

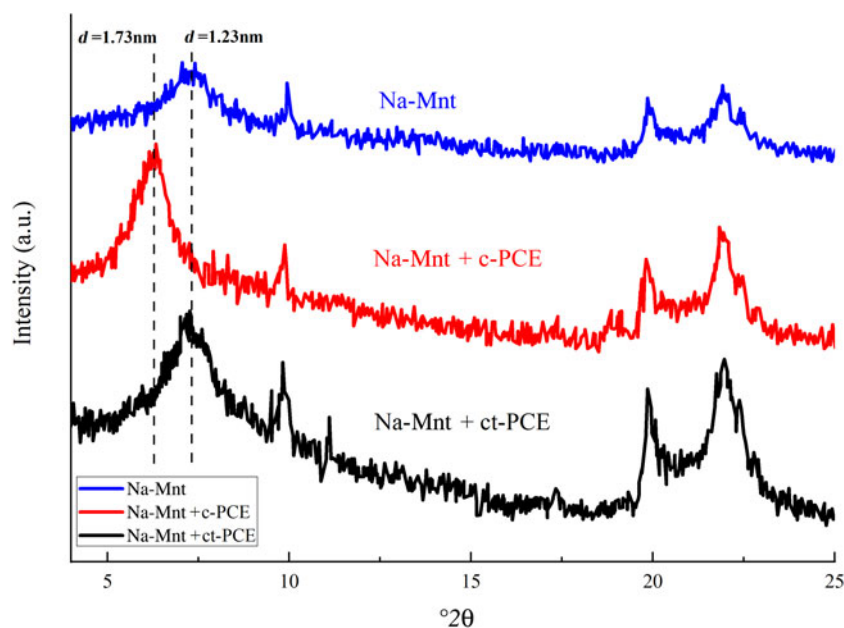


Fig. 6. XRD traces of Na-Mnt with or without PCE.

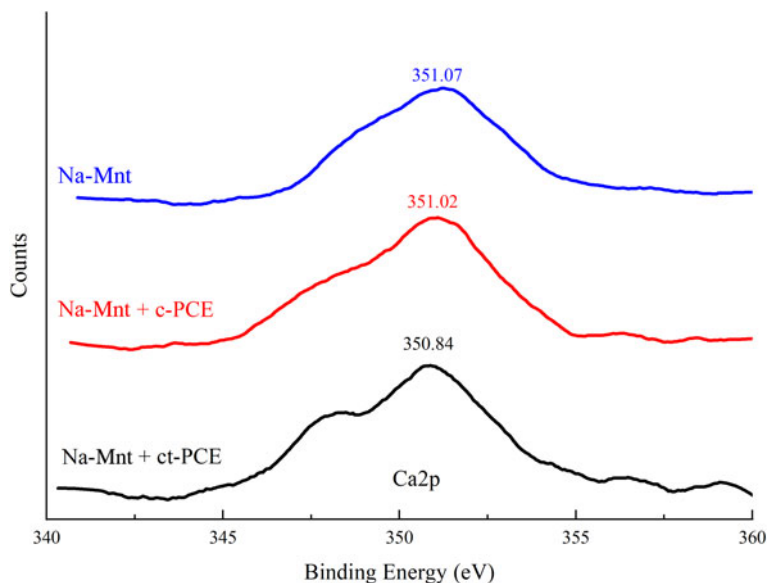


Fig. 7. Binding-energy spectrum of calcium in PCE-Mnt.

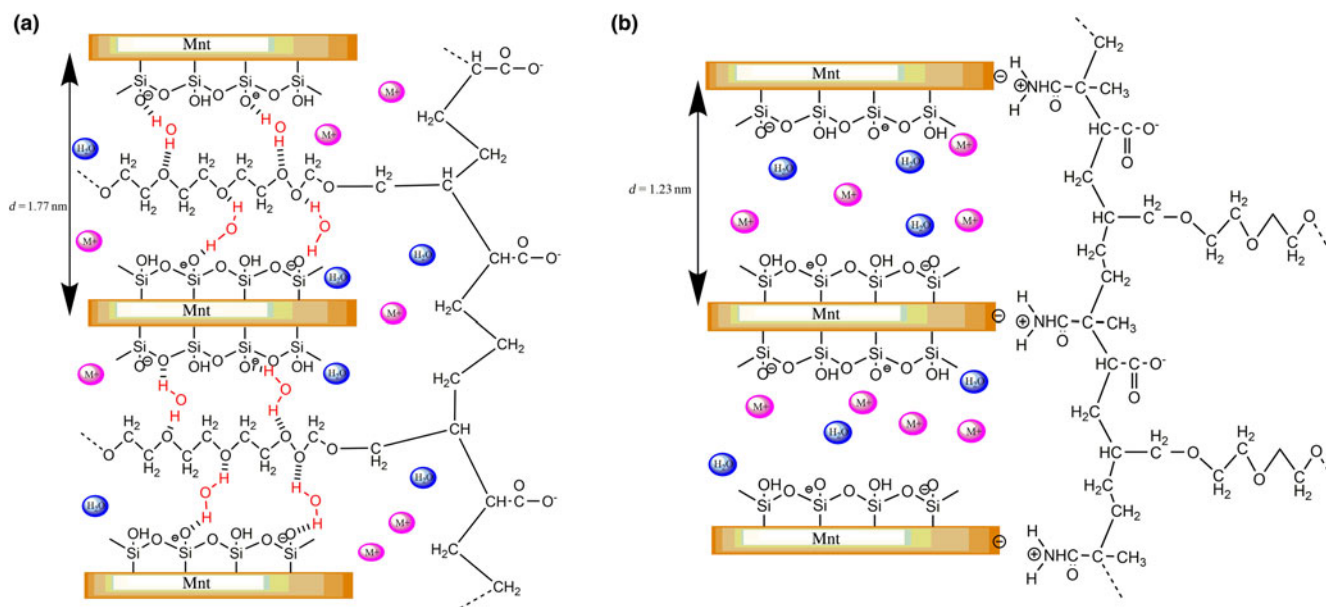


Fig. 8. Schematic diagram of Mnt with PCEs: (a) c-PCE and (b) ct-PCE.

Photoelectron intensity was less in the samples supplied with PCEs than in pure Na-Mnt, indicating that the PCEs were adsorbed on the surface of Na-Mnt. The thickness of the new

Table 4. Si2p data of XPS and thickness of the sorption layer of PCE on Na-Mnt.

	Na-Mnt	ct-PCE	c-PCE
$h\nu$ (eV)	1486.6		
Eb (eV)	102.89	102.51	102.56
Counts of the peak height	15,207.92	14,543.82	14,030.81
FWHM (eV)	1.76	1.98	1.9
$I_0$	33,310.34		
$I(b)$		25,310.34	30,245.11
Thickness (nm)		1.12	0.39

Eb = electron binding energy; FWHM = peak width at half-height;  $h\nu$  = photoelectron kinetic energy;  $I_0$  = initial photoelectron intensity;  $I(b)$  = photoelectron intensity after the photoelectron goes through the adsorption layer.

ct-PCE was calculated as 1.12 nm, while that of the adsorption layer was only 0.39 nm, which can be attributed to the dispersed side-chain in the solution rather than to intercalation between Na-Mnt layers. The increased adsorption layer again indicated that no intercalation of the side-chain of ct-PCE occurred.

The adsorption of PCEs in a cement system depends on  $\text{Ca}^{2+}$  (Tan *et al.*, 2018b). The bond energy spectra of  $\text{Ca}^{2+}$  on the PCE-superplasticized Na-Mnt are shown in Fig. 7. The XPS spectrum revealed that not only does adsorption occur between the cement and PCEs, but there were also some chemical interactions with the dissolved ions. In comparison with pure Na-Mnt (351.07 eV), the binding energies of Ca2p in the presence of ct-PCE and c-PCE were 350.84 and 351.04 eV, respectively, which are close to that of pure Na-Mnt. This result indicated that new types of  $\text{Ca}^{2+}$  compounds did not form in the sample.

### Model of interaction between PCE and Na-Mnt

The Mnt has a 2:1 structure with water and cations occupying the interlayer space (Fig. 8). Upon contact with water, Mnt layers swell due to expansion of the interlayer volume. Water molecules can enter the interlayers and cations within the interlayer space exchange with cations in the solution. The  $d_{001}$  spacing of the original Mnt varied between 1.20 and 1.90 nm depending on the type of interlayer cations (Ait-Akbour *et al.*, 2015). As PCE is larger than the interlayer space, the polymer cannot easily enter the interlayer space and instead is adsorbed on the Mnt surface due to electrostatic attraction (Table 4). The side-chain of the PCE may also intercalate between the layers.

In the presence of c-PCE, the  $d_{001}$ -spacing of Mnt increased from ~1.23 to 1.73 nm. The increased spacing between layers suggests that the PEO side-chain of the c-PCE entered the interlayer of Na-Mnt. The conformation size of the PEO side-chain in solution is ~0.70–1.40 nm (Houst *et al.*, 2008), which is less than the interlayer space; hence, the PEO side-chain may enter the Mnt. As discussed in the 'Sorptions of PCE on Na-Mnt' section, a much greater sorption of c-PCE in Na-Mnt was observed, but the dispersion ability was still poor. This suggests that, compared to sorption, intercalation by the PEO side-chain was the dominant mechanism for c-PCE in Na-Mnt. Compared to ct-PCE, the smaller thickness of the sorbed PCE layer also indicates that intercalation of the PEO side-chain occurred in the presence of c-PCE (Table 4).

The conformation size of the ct-PCE was ~5.25 nm, which was larger than the spacing between the layers (1.23 nm) (Table 3). The 001 peak of Mnt did not shift with the addition of ct-PCE, indicating that no intercalation of ct-PCE occurred in the interlayer space (Fig. 6). This may be because the introduced cationic groups inhibited the expansion of Na-Mnt and consequently reduced the likelihood of intercalation by PEO. Lower sorption appears to enhance ct-PCE dispersion performance, which indicates that the new terpolymer is clay-tolerant.

### Conclusions

The results of this work are summarized as follows:

- (1) Introducing cationic amide groups with shorter side-chain lengths improved the dispersion performance of PCE in cement containing Na-Mnt by increasing the initial minislump of the cement paste.
- (2) A quadratic model for the minislump of the cement pastes mixed with Na-Mnt was developed statistically. The optimal conditions for ct-PCE dispersion performance in Na-Mnt-incorporated cement paste were a side-chain ratio ((AA + AM):APEG) of 4:9, a monomer ratio (AA:AM) of 9:8, an initiator dosage of 2.9% and a synthesis temperature of 81°C. Experimental values confirmed the optimization accuracy of the model.
- (3) The dosage requirement of both ct-PCE and c-PCE increased as the Na-Mnt dosage increased. Compared to commercial c-PCE, the modified ct-PCE showed a lower dosage requirement.
- (4) Unlike commercial PCE, no intercalation occurred in the newly manufactured ct-PCE with clay, leading to better cement dispersion.

Although the ct-PCE was successfully synthesized and its compatibility with Na-Mnt was investigated in this study, a

comprehensive understanding of the mechanism was not achieved. Further research is necessary.

**Acknowledgements.** Mr Shengye Xu is acknowledged for his contribution to this manuscript.

**Financial support.** Financial support from the National Natural Science Foundation of China including 51908526 (Jun Ren), 51808196 (Shuqiong Luo), 51772227 (Hongbo Tan) and 52008256 (Min Liu), and from College Student Innovation and Entrepreneurship Training Project of Yunnan University (202105091, Jun Ren), is gratefully acknowledged.

### References

- Ait-Akbour R., Boustingorry P., Leroux F., Leising F. & Taviot-Guého C. (2015) Adsorption of polycarboxylate poly(ethylene glycol) (PCP) esters on montmorillonite (Mnt): effect of exchangeable cations ( $\text{Na}^+$ ,  $\text{Mg}^{2+}$  and  $\text{Ca}^{2+}$ ) and PCP molecular structure. *Journal of Colloid and Interface Science*, **437**, 227–234.
- Chen G., Lei J., Du Y., Du X. & Chen X. (2018) A polycarboxylate as a superplasticizer for montmorillonite clay in cement: adsorption and tolerance studies. *Arabian Journal of Chemistry*, **11**, 747–755.
- Dziekani E., Laska J. & Małolepszy J. (2011) Influence of polymer superplasticizers on the properties of autoclaved aerated concrete. *Cement Wapno Beton*, 34–38.
- Flatt R.J. & Houst Y.F. (2001) A simplified view on chemical effects perturbing the action of superplasticizers. *Cement and Concrete Research*, **31**, 1169–1176.
- Gao G.B., Ren J., Liu Y., Guo J.Y. & Li J. (2018) Interaction of polycarboxylate-based superplasticiser with clay in Portland cement systems. *Advances in Cement Research*, **30**, 270–276.
- Guo Y.X., Liu J.H., Gates W.P. & Zhou C.H. (2020) Organo-modification of montmorillonite. *Clays and Clay Minerals*, **68**, 601–622.
- Houst Y.F., Bowen P., Perche F., Kauppi A., Borget P., Galmiche L. *et al.* (2008) Design and function of novel superplasticizers for more durable high performance concrete (superplast project). *Cement and Concrete Research*, **38**, 1197–1209.
- Ioannidou D., Meylan G., Sonnemann G. & Habert G. (2017) Is gravel becoming scarce? Evaluating the local criticality of construction aggregates. *Resources, Conservation and Recycling*, **126**, 25–33.
- Ji D., Luo Z., He M., Shi Y. & Gu X. (2012) Effect of both grafting and blending modifications on the performance of lignosulphonate-modified sulphonic acid-phenol-formaldehyde condensates. *Cement and Concrete Research*, **42**, 1199–1206.
- Lei L. & Plank J. (2012a) A concept for a polycarboxylate superplasticizer possessing enhanced clay tolerance. *Cement and Concrete Research*, **42**, 1299–1306.
- Lei L. & Plank J. (2012b) Synthesis, working mechanism and effectiveness of a novel cycloaliphatic superplasticizer for concrete. *Cement and Concrete Research*, **42**, 118–123.
- Lei L. & Plank J. (2014a) A study on the impact of different clay minerals on the dispersing force of conventional and modified vinyl ether based polycarboxylate superplasticizers. *Cement and Concrete Research*, **60**, 1–10.
- Lei L. & Plank J. (2014b) Synthesis and properties of a vinyl ether-based polycarboxylate superplasticizer for concrete possessing clay tolerance. *Industrial & Engineering Chemistry Research*, **53**, 1048–1055.
- Li Y., Zheng X., Wu K. & Lu M. (2016) Synthesis of amphiphilic polycarboxylate copolymer and its notable dispersion and adsorption characteristics onto cement and clay. *Advances in Cement Research*, **28**, 344–353.
- Li C., Wu Q., Petit S., Gates W.P., Yang H., Yu W. & Zhou C. (2019) Insights into the rheological behavior of aqueous dispersions of synthetic saponite: effects of saponite composition and sodium polyacrylate. *Langmuir*, **35**, 13040–13052.
- Liu X., Guan J., Lai G., Zheng Y., Wang Z., Cui S. *et al.* (2017) Novel designs of polycarboxylate superplasticizers for improving resistance in clay-contaminated concrete. *Journal of Industrial and Engineering Chemistry*, **55**, 80–90.
- Ma Y., Shi C., Lei L., Sha S., Zhou B., Liu Y. & Xiao Y. (2020) Research progress on polycarboxylate based superplasticizers with tolerance to clays – a review. *Construction and Building Materials*, **255**, 119386.



- Nehdi M.L. (2014) Clay in cement-based materials: critical overview of state-of-the-art. *Construction and Building Materials*, **51**, 372–382.
- Ng S. & Plank J. (2012) Interaction mechanisms between Na montmorillonite clay and MPEG-based polycarboxylate superplasticizers. *Cement and Concrete Research*, **42**, 847–854.
- Ran Q.P., Somasundaran P., Miao C.W., Liu J.P., Wu S.S. & Shen J. (2009) Effect of the length of the side chains of comb-like copolymer dispersants on dispersion and rheological properties of concentrated cement suspensions. *Journal of Colloid and Interface Science*, **336**, 624–633.
- Rashad A.M. (2018) Lightweight expanded clay aggregate as a building material – an overview. *Construction and Building Materials*, **170**, 757–775.
- Ren J., Fang Y., Ma Q., Tan H., Luo S., Liu M. & Wang X. (2019) Effect of storage condition on basic performance of polycarboxylate superplasticiser system incorporated sodium gluconate. *Construction and Building Materials*, **223**, 852–862.
- Ren J., Wang X., Xu S., Fang Y., Liu W., Luo Q. *et al.* (2021) Effect of polycarboxylate superplasticisers on the fresh properties of cementitious materials mixed with seawater. *Construction and Building Materials*, **289**, 123143.
- Sánchez-Martín M.J., Dorado M.C., Hoyo C.D. & Rodríguez-Cruz M.S. (2008) Influence of clay mineral structure and surfactant nature on the adsorption capacity of surfactants by clays. *Journal of Hazardous Materials*, **150**, 115–123.
- Shen C.C., Petit S., Li C.J., Li C.S., Khatoun N. & Zhou C.H. (2020) Interactions between smectites and polyelectrolytes. *Applied Clay Science*, **198**, 105778.
- Sun Z., Yang H., Shui L., Liu Y., Yang X., Ji Y. *et al.* (2016) Preparation of polycarboxylate-based grinding aid and its influence on cement properties under laboratory condition. *Construction and Building Materials*, **127**, 363–368.
- Suter J.L. & Coveney P.V. (2009) Computer simulation study of the materials properties of intercalated and exfoliated poly(ethylene)glycol clay nanocomposites. *Soft Matter*, **5**, 2239–2251.
- Tambach T.J., Hensen E.J.M. & Smit B. (2004) Molecular simulations of swelling clay minerals. *Journal of Physical Chemistry B*, **108**, 7586–7596.
- Tan H., Gu B., Ma B., Li X., Lin C. & Li X. (2016a) Mechanism of intercalation of polycarboxylate superplasticizer into montmorillonite. *Applied Clay Science*, **129**, 40–46.
- Tan H., Zou F., Ma B., Liu M., Li X. & Jian S. (2016b) Effect of sodium tripolyphosphate on adsorbing behavior of polycarboxylate superplasticizer. *Construction and Building Materials*, **126**, 617–623.
- Tan H., Guo Y., Ma B., Huang J., Gu B. & Zou F. (2018b) Effect of sodium tripolyphosphate on clay tolerance of polycarboxylate superplasticizer. *KSCE Journal of Civil Engineering*, **22**, 2934–2941.
- Tang X., Zhao C., Yang Y., Dong F. & Lu X. (2020) Amphoteric polycarboxylate superplasticizers with enhanced clay tolerance: preparation, performance and mechanism. *Construction and Building Materials*, **252**, 119052.
- Tan H., Gu B., Guo Y., Ma B., Huang J., Ren J. *et al.* (2018a) Improvement in compatibility of polycarboxylate superplasticizer with poor-quality aggregate containing montmorillonite by incorporating polymeric ferric sulfate. *Construction and Building Materials*, **162**, 566–575.
- Tan H., Li M., Ren J., Deng X., Zhang X., Nie K. *et al.* (2019) Effect of aluminum sulfate on the hydration of tricalcium silicate. *Construction and Building Materials*, **205**, 414–424.
- Tregger N.A., Pakula M.E. & Shah S.P. (2010) Influence of clays on the rheology of cement pastes. *Cement and Concrete Research*, **40**, 384–391.
- Wala D. & Rosiek G. (2003) Minerály ilaste jako dodatek pucolanowy do cementów hydraulicznych. *Cement Wapno Beton*, **8**, 27–33.
- Wang W., Deng Z., Feng Z., Fu L. & Zheng B. (2015) Interaction of polycarboxylate-based superplasticizer/poly(vinyl alcohol) with bentonite and its application in mortar with clay-bearing aggregates. *ACI Symposium Publication*, **302**, 333–348.
- Wang X.F., Fang C., Kuang W.Q., Li D.W., Han N.X. & Xing F. (2017) Experimental study on early cracking sensitivity of lightweight aggregate concrete. *Construction and Building Materials*, **136**, 173–183.
- Warr L.N. (2020) Recommended abbreviations for the names of clay minerals and associated phases. *Clay Minerals*, **55**, 261–264.
- Xing G., Wang W. & Xu J. (2016) Grafting tertiary amine groups into the molecular structures of polycarboxylate superplasticizers lowers their clay sensitivity. *RSC Advances*, **6**, 106921–106927.
- Xu H., Sun S., Yu Q. & Wei J. (2018) Effect of  $\beta$ -cyclodextrin pendant on the dispersion robustness of polycarboxylate superplasticizer toward kaolin. *Polymer Composites*, **39**, 755–761.
- Zadaka D., Radian A. & Mishael Y.G. (2010) Applying zeta potential measurements to characterize the adsorption on montmorillonite of organic cations as monomers, micelles, or polymers. *Journal of Colloid and Interface Science*, **352**, 171–177.
- Zhang Y., Liu H.Q., Tong R.M. & Ren J. (2019) Effect of nano silica on freeze-thaw resistance of cement-fly ash mortars, cured in corrosive condition at different temperature. *Cement Wapno Beton*, **24**, 137–153.
- Zhang J.R., Xu M.D., Christidis G.E. & Zhou C.H. (2020) Clay minerals in drilling fluids: functions and challenges. *Clay Minerals*, **55**, 1–11.
- Zhao H., Wang Y., Yang Y., Shu X., Yan H. & Ran Q. (2017) Effect of hydrophobic groups on the adsorption conformation of modified polycarboxylate superplasticizer investigated by molecular dynamics simulation. *Applied Surface Science*, **407**, 8–15.